International Journal of Pharmaceutics, 17 (1983) 237–262
Elsevier

Desolvation kinetics of cefamandole sodium methanolate: the effect of water vapor

M.J. Pikal, J.E. Lang and S. Shah

Lilly Research Laboratories, Eli Lilly and Company, Indianapolis, IN 46285 (U.S.A.)

(Received December 3rd, 1982)
(Modified version May 13th, 1983)
(Accepted May 16th, 1983)

Summary

Processing of crystalline pharmaceuticals often involves removal of the solvent of crystallization. Several cases are documented where removal of solvated alcohol is much faster when the sample is simply exposed to ambient humidity than when the sample is vacuum-dried. The most dramatic example of this phenomenon occurs with the methanolate of cefamandole sodium. Cefamandole sodium may exist in 1 of 3 crystalline forms giving different X-ray powder patterns: methanolate, hydrate, or anhydrate. This research is a detailed phenomenological study of the kinetics and thermodynamics of the desolvation and solvation reactions of cefamandole sodium. The effects of water vapor, temperature, sample history, and crystal size are experimentally evaluated. The phenomenological generalizations are employed to develop a mechanistic interpretation of the data. The methanolate of cefamandole sodium exhibits some characteristics of a non-stoichiometric solvate and has a solvation enthalpy 3.7 kcal/mol greater than the enthalpy of condensation of the solvent. The rate of vacuum demethanolation increases sharply as the crystal size decreases; is as much as a factor of 200 slower than demethanolation in the presence of water vapor; yields an apparent activation energy equal to the enthalpy of reaction; and is apparently limited by mass transfer of the methanol through the low permeability anhydrate phase. Demethanolation in the presence of water vapor yields a hydrate which, as a first approximation, is a non-stoichiometric solvate. Dehydration of the hydrate is rapid. The much faster rate of conversion of methanolate to hydrate is largely a result of the extensive crystal cracking and subsequent reduction of effective crystal size which occurs during the early stages of

Correspondence: M.J. Pikal, Lilly Research Laboratories, 307 East McCarty Street, Indianapolis, IN 46285, U.S.A.

0378-5173/83/$03.00

hydrate formation. However, it also appears that the hydrate phase is more permeable to methanol than is the anhydrate phase.

Introduction

Desolvation reactions are often involved in the processing of crystalline pharmaceuticals, and it is frequently necessary to reduce residual solvents to very low levels to avoid stability problems and/or toxicity of the solvent. Desolvation is commonly accomplished by vacuum-drying, and from our observations, may require drying times that are both long and quite variable between different lots of the same product. A particularly curious observation, illustrated by Scheme I, is that in

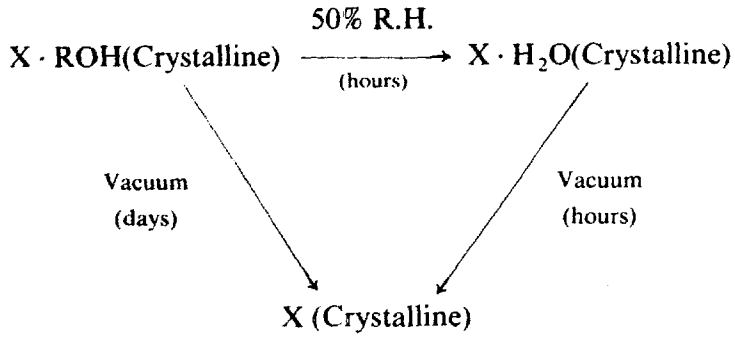

Scheme I

several cases, solvated alcohol can be removed much faster by simply exposing a sample to ambient humidity than by vacuum-drying. Exposure of the sample to roughly 50% relative humidity (R.H.) quickly converts the alcohol solvate to a material which, in chemical composition, is a hydrate. The hydrate may then be easily converted to the anhydrate (X) by drying in either vacuum or dry air. This phenomenon (Scheme I) is observed for 3 cephalosporins: cefamandole sodium methanolate, cefamandole nafate methanolate, and the pseudo-ethanol solvate [1] of cefazolin sodium. Cefamandole sodium appears to be the most dramatic demonstration of the acceleratory effect of water vapor on demethanolation. Removal of methanol (< 0.2% w/w) by conversion to the hydrate followed by removal of water (< 0.2% w/w) requires only about 6 h at 25°C while the corresponding time required to form the anhydrate via vacuum-drying (25°C) may exceed 1 month.

While it is unlikely that the cephalosporins studied in this research are the only examples of Scheme I, there appear to be no direct parallels in the literature. However, several examples of the acceleratory effect of water vapor on solid state endothermic reactions are well documented (Young, 1966). Rates of dehydration of

[1] Cefazolin sodium forms a hydrate (α-form) which when exposed to ethanol will partially exchange water for ethanol. See the experimental section for more detail.

inorganic hydrates frequently pass through maxima as the partial pressure of water increases. This phenomenon, referred to as the Smith-Topley effect, is attributed to the formation of a low permeability amorphous product at low partial pressures of water but crystallization to a more permeable crystalline product at higher partial pressures. The decomposition of carbonates also proceeds faster in the presence of water vapor (Young, 1966), a result interpreted by postulating blockage of product CO_2 adsorption at active sites by water adsorption, thereby increasing the rate of CO_2 removal.

The primary objective of this research is to present a detailed phenomenological study of the kinetics and thermodynamics of the desolvation reactions of cefamandole sodium, specifically addressing the effects of water vapor, temperature, sample history, and crystal size. Secondly, the phenomenological generalizations are used to justify a mechanistic interpretation of the data. Progress of the following reactions involving cefamandole sodium (NaCM) was studied gravimetrically:

(A)	$NaCM \cdot CH_3OH(s) \rightarrow$	$NaCM(s) + CH_3OH(v)$
(B)	$NaCM(s) + CH_3OH(v) \rightarrow$	$NaCM \cdot CH_3OH(s)$
(C)	$NaCM \cdot CH_3OH(s) + H_2O(v) \rightarrow$	$NaCM \cdot H_2O(s) + CH_3OH(v)$
(D)	$NaCM \cdot H_2O(s) + CH_3OH(v) \rightarrow$	$NaCM \cdot CH_3OH(s) + H_2O(v)$
(E)	$NaCM \cdot H_2O(s) \rightarrow$	$NaCM(s) + H_2O(v)$

In addition, desorption/absorption isotherms were determined to evaluate the equilibrium vapor pressures of both the methanolate and hydrate forms, and calorimetric heats of reaction were determined for reactions A, C and E.

Experimental

Materials

Cefamandole sodium methanolate is prepared in the laboratory by slow addition of a methanol solution of sodium acetate to a methanol solution of purified cefamandole acid. The solution is allowed to stand at room temperature for several hours before harvesting the crystals. The resulting crystals are separated from the mother liquor by filtration, washed first with ethanol and then with ether, and finally vacuum-dried for several hours at room temperature to remove ether. Lots no. 2, 3 and 5 were prepared in this manner. Lots no. 1 and 4 were obtained from production scale preparations using nominally the same general procedure without the ether wash. The resulting crystals were, however, much smaller in size. All crystals were stored in sealed tubes at room temperature after equilibration at 25°C with methanol vapor at a partial pressure of 10 mm Hg. The bulk samples were re-equilibrated with methanol vapor after each sample withdrawal. Microscopic examination showed that the crystals retained their initial appearance when stored in this manner.

Cefamandole nafate methanolate is crystallized by addition of a methanol solution of sodium 2-ethyl hexanoate to a methanol solution of cefamandole nafate acid. The resulting crystals are separated from mother liquor by filtration, washed with isopropyl alcohol, and filtered to yield a wet cake containing the methanolate and roughly 50% isopropyl alcohol. Methanol sorption isotherms suggest the crystals which first form contain two moles of methanol per mole of cefamandole nafate. Evidently, the isopropyl alcohol wash removes at least one mole of methanol easily, normally leaving the mole ratio of methanol to cefamandole nafate slightly less than 1 : 1.

The pseudo-ethanol solvate of cefazolin sodium is prepared by exposing the α-form crystals, normally referred to as pentahydrate (Pikal et al., 1978), to ethanol via a prolonged wash of the crystals with ethanol. The resulting wet cake is then vacuum-dried at room temperature for several hours to remove liquid state ethanol. The pentahydrate is more properly described as a non-stoichiometric hydrate. Evidently, the crystals undergo partial dehydration in the presence of ethanol with accompanying substitution of ethanol for some of the water removed. The crystals obtained are, therefore, referred to as a pseudo-ethanol solvate.

Reagent grade methanol, dried over 3A molecular sieve, water for injection [2], and nitrogen (99.9%) were used as supplied. The cephalosporin acid and cefazolin sodium were obtained as chemical intermediates [2].

Calorimetry / X-ray

Heats of solution and X-ray diffraction patterns were obtained using previously described equipment and procedures (Pikal et al., 1978).

Microscopic observations

Microscopic observations of crystals during demethanolation in vacuum were made using a high vacuum temperature-controlled microscope stage originally designed for observation of freeze-drying (Pikal et al., 1983). In the freeze-drying application, cold nitrogen gas is circulated through the device to maintain sub-ambient temperature. For the present application, temperature control above ambient temperature is accomplished by circulating thermostatically controlled water.

Kinetic studies

Apparatus / procedures

The mass change resulting from the desolvation, solvation or solvent exchange reaction was determined using a high vacuum electronic microbalance [3] (Pikal et al., 1983) with output monitored as a function of time on a strip chart recorder. The apparatus used for vacuum demethanolation studies (Fig. 1A) consists of the microbalance and thermostats for maintaining the sample at temperature T_1 and the methanol at temperature T_2. A small amount of 3A molecular sieve is placed in the

[2] Eli Lilly.

[3] Sartorius Model 4102.

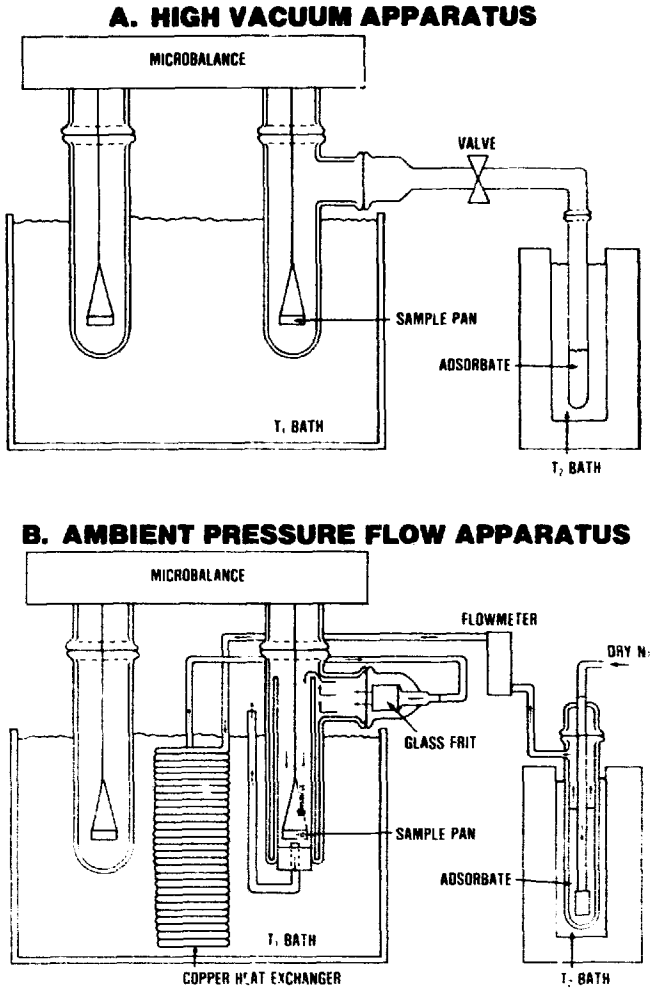

Fig. 1. Apparatus for kinetic studies.

methanol to minimize extraneous moisture effects. A sample (100 mg) is placed in a 1.5 cm diameter quartz bucket (300 mg) forming a powder bed roughly 1.5 mm deep. Prior to an experiment, the sample is equilibrated with methanol vapor at a pressure fixed by T_2. The system is evacuated with the methanol at liquid nitrogen temperature. The pumping system is valved off, and the methanol is brought to temperature T_2. Transfer of methanol vapor between the T_2 bath and the sample proceeds until equilibrium is established at which point the sample mass is independent of time. The desolvation experiment is started by closing the valve between the sample and the methanol and opening the microbalance system to the pumping system.

An ambient pressure vapor flow apparatus, utilizing the same microbalance, is used to study all reactions where nitrogen gas was passed over the sample (Fig. 1B). Here, the sample (100 mg) is placed in a 1 cm diameter aluminum bucket (30 mg). Dry nitrogen at a flow rate of 100 ml · min^{-1} is passed through a glass frit immersed in the adsorbate liquid at temperature T_2, through a flowmeter, through a heat exchanger to bring the vapor to temperature T_1, and finally into the sample chamber

(Fig. 1B). For studies with pure nitrogen (desolvations at zero relative humidity), dry nitrogen was passed directly into the flowmeter. As with the vacuum studies, the sample is equilibrated with the appropriate vapor at the selected vapor pressure before an experiment, and after equilibration, the experiment is started by switching adsorbate tubes. For example, equilibration with methanol is followed by quickly connecting an adsorbate tube containing water at the appropriate temperature to initiate the methanol–water exchange reaction.

In all studies, the fractional extent of the reaction being studied at any given time is defined as the mass change at that time divided by the mass change at infinite time (equilibrium). Chemical composition and X-ray diffraction patterns were only obtained before and after an experiment to verify the nature of the starting material and product. Thus, the kinetic data are based solely on gravimetric results.

Self-cooling

Due to the heat requirement for desolvation, self-cooling of the sample is a potential problem (Anous et al., 1951; Barrer, 1948). While temperature differences within a crystal are negligible (Anous et al., 1951), the crystals may be significantly lower in temperature than the bath (or thermostat) temperature. Consequently, two different experiments were carried out to assess the magnitude of the self-cooling effect for vacuum demethanolation. First, the effect of air pressure on the pseudo-first-order rate constant for demethanolation at 40.8°C was examined from 10^{-6} mm Hg to 470 mm Hg. Using the vacuum apparatus configuration (Fig. 1A) with temperature T_2 at 78 K to serve as a sink for methanol, the air pressure is reduced step-wise to allow the rate of mass loss to be evaluated at each pressure studied. The basic premise of this experiment is that while in high vacuum, heat transfer from the thermostat to the sample is only by radiative heat flow. However, additional heat transfer mechanisms (conduction and possibly convection) become significant at higher pressure. Thus, the degree of self-cooling should be much less at pressures greater than several mm Hg (Anous et al., 1951) where the conduction effect should reach its maximum (Pikal et al., 1983). However, at high pressures, the reaction rate may be in part, determined by gas phase diffusion of the methanol from the sample to the sink (T_2 bath) (Birks and Bradley, 1949). Since the diffusional resistance is directly proportional to pressure, one might expect that, at high pressures, the reciprocal of the observed rate constant will be a linear function of pressure where the zero pressure intercept is the reciprocal of the pseudo-first-order rate constant for the desolvation reaction under conditions of high heat transfer and correspondingly low self-cooling.

Experimentally, the *reciprocal* of the rate constant is linear in pressure at pressures above 1 mm Hg, the rate constant itself decreasing by about 25% between 1 mm Hg and 470 mm Hg. The zero pressure intercept yields an extrapolated rate constant which is about 10% ($\pm 4\%$) higher than the rate constant observed at 10^{-6} mm Hg, suggesting a modest but significant self-cooling effect in high vacuum. With an activation energy of 12 kcal/mol, the calculated self-cooling effect is 1.5°C (± 0.6°C) in vacuum, assuming the self-cooling effect above 1 mm Hg is negligible.

The second experiment involves measuring the rate of heat transfer to a sample

by suddenly changing the bath temperature and following the sample temperature, T, as a function of time, t, by measuring the rate of mass loss as a function of time. If a sample originally at T_0 is placed in a bath of temperature T_b, the sample will gain (or lose) heat according to the energy balance.

$$\dot{Q}_c + \dot{Q}_v = \dot{Q}_B \tag{1}$$

where $\dot{Q}_c$ is the rate of heat gain (or loss) of the sample of total heat capacity C

$$\dot{Q}_c = C\frac{dT}{dt} \tag{2}$$

$\dot{Q}_v$ is the heat loss rate by desolvation,

$$\dot{Q}_v = n\Delta\bar{H}^0 \cdot \frac{d\alpha}{dt} \tag{3}$$

for n moles of sample where the enthalpy of desolvation is $\Delta\bar{H}^0$ and α is the fractional extent of the reaction, and $\dot{Q}_B$ is the rate of heat transfer to the sample from the bath,

$$\dot{Q}_B = k_t(T_b - T) \tag{4}$$

where k_t is a heat transfer coefficient. Except for long times where the sample is close to steady-state, the magnitude of $\dot{Q}_v$ is much smaller than the other terms in Eqn. 1 and may be neglected. Denoting the temperature difference between bath and sample by ΔT ($= T_b - T$), Eqns. 1, 2 and 4 may be combined and integrated with the boundary condition, $\Delta T(t = 0) = \Delta T_0 = T_b - T_0$, to give

$$\ln(\Delta T/\Delta T_0) = -(k_t/C)t \tag{5}$$

Since the rate of desolvation is sensitive to temperature, desolvation rate can serve as a sample thermometer. Assuming the usual Arrhenius expression for rate of mass loss, $\dot{m}$,

$$\dot{m} = A\exp(-E^*/RT) \tag{6}$$

where A is the preexponential constant, E^* is the apparent activation energy, R is the gas constant, and T is the sample temperature (K), which is time dependent. Therefore, the ratio of temperature differences needed to evaluate the lefthand side of Eqn. 5 may be written

$$\frac{\Delta T}{\Delta T_0} = \frac{\ln(\dot{m}(\infty)/\dot{m}(t))}{\ln(\dot{m}(\infty)/\dot{m}(0))} \cdot \frac{T}{T_0}. \tag{7}$$

Here, $\dot{m}(0)$ denotes the rate of mass loss before the bath temperature change, $\dot{m}(\infty)$ is the steady-state rate after the temperature change (roughly independent of time),

and $\dot{m}(t)$ is the strongly time-dependent rate measured while the sample is changing temperature. While the rates are experimentally measurable, the sample temperature, T, cannot be directly measured. However, the logarithmic term varies by roughly a factor of 10 during the experiment while the term T/T_0 changes only by about 12%. Further, in heating, $T/T_0 > 1$, while in cooling, $T/T_0 < 1$. Thus, defining $(\Delta T/\Delta T_0)_m$ as the mean of $\Delta T/\Delta T_0$ data (at a given time) for the heating and cooling modes of an experiment between the same two bath temperatures, the effect of the ratio T/T_0 will mostly cancel and we may write

$$\left(\frac{\Delta T}{\Delta T_0}\right)_m \cong \frac{\ln[\dot{m}(\infty)/\dot{m}(t)]}{\ln[\dot{m}(\infty)/\dot{m}(0)]} \tag{8}$$

Since Eqn. 5 applies equally well for the mean temperature difference ratio, $(\Delta T/\Delta T_0)_m$, the lefthand side of Eqn. 5 is determined from experimental mass loss data as a function of time via Eqn. 8.

In the experiment, a 150 mg sample was exposed to the temperatures: 27.2°C, 64.7°C, 27.2°C; and the rate of mass loss was evaluated as a function of time during the experiment. The heat capacity of the system, C (0.10 cal/°C), is assumed to be the sum of the heat capacity of the quartz pan (0.06 cal/°C) and the heat capacity of the sample (0.04 cal/°C). The data were fit to Eqn. 5 with $\Delta T/\Delta T_0$ given by Eqn. 8, which yields, with $C = 0.1$ cal/°C, $k_t = 7.3 \times 10^{-4}$ cal $\cdot s^{-1} \cdot °C^{-1}$. Theoretical calculation of k_t using unit emissivity gives 10.5×10^{-4} cal $\cdot s^{-1} \cdot °C^{-1}$, a result in excellent agreement with the experimental value.

At steady-state, the temperature error due to self-cooling may be calculated by the relation, $\dot{Q}_v = \dot{Q}_B$ where $\dot{Q}_v$ and $\dot{Q}_B$ are given by Eqns. 3 and 4, respectively. At 40°C, the calculated self-cooling effect is on the order of 0.1°C when desolvating a fully solvated sample. This result indicates the self-cooling effect for demethanolation in vacuum is negligible, a conclusion contrary to the interpretation given the pressure dependence studies described earlier, where a self-cooling effect on the order of 1°C was estimated. While both experiments are susceptible to systematic error, the self-cooling effect estimated from the temperature change experiment is probably less sensitive to such error and, therefore, is perhaps the more reliable estimate. However, as a precaution, the experiment designed to measure the apparent activation energy for demethanolation is carried out at a background air pressure of 2 mm Hg to minimize any self-cooling effect.

The self-cooling effect for a sample in a stream of nitrogen may be estimated using the steady-state approximation, $\dot{Q}_v = \dot{Q}_B$ where $\dot{Q}_v$ and $\dot{Q}_B$ are given by Eqns. 3 and 4, respectively. However, the heat transfer coefficient, k_t, now includes heat transfer by gas conduction and forced convection (i.e. flowing nitrogen) as well as radiation. Due to the smaller size and lower emissivity of the aluminum sample pan used in high vacuum studies, the radiative heat transfer coefficient is estimated to be about a factor of 5 less, or 1.5×10^{-4} cal $\cdot s^{-1} \cdot °C^{-1}$. From the dimensions of the system and the thermal conductivity of N_2 (Dushman, 1962), the contribution of gas conduction to k_t is estimated as 3×10^{-4} cal $\cdot s^{-1} \cdot °C^{-1}$. The contribution of forced convection to k_t is proportional to the nitrogen flow rate, $\dot{v}$ (l/min). Using

handbook data for the specific heat of nitrogen the convective contribution to k_t is 47×10^{-4} v cal · s · °C^{-1}. Thus the estimated value of k_t is 9.2×10^{-4} cal · s^{-1} · °C^{-1} at 0.1 l/min.

For the methanolate to hydrate conversion, the heat of reaction is nearly zero and $\dot{Q}_v$ is essentially zero. Thus, we expect no self-cooling for this reaction. Experimentally, the rate of reaction does not change on reducing the N_2 flow rate from 0.1 to 0.05 l/min, a result consistent with this conclusion.

The hydrate to anhydrate reaction is both strongly endothermic ($\Delta H \cong 12$ kcal/mol) and rapid (half-life ~ 0.25 h). Here, the self-cooling is estimated as 2.0°C for a flow rate of 0.1 l/min and 2.7°C for a flow rate of 0.05 l/min. Experimentally, the dehydration rate decreases by about 40% on reducing the N_2 flow rate from 0.1 to 0.05 l/min. The rate reduction of 40% is larger than expected from the self-cooling effect alone and probably reflects, in part, an increase in stagnant gas layer thickness at the boundary between the powder and the moving nitrogen.

Desorption / absorption isotherms

For a given sample, the desorption isotherm is determined first, followed by determination of the absorption isotherm. Using either the high vacuum apparatus or the ambient pressure flow apparatus (Fig. 1), the temperature of the T_2 bath is varied stepwise to produce stepwise changes in solvent partial pressure. Following a step change in partial pressure, the sample mass is recorded as a function of time until the mass becomes invarient with time, indicating equilibrium conditions have been reached. The absorption/desorption isotherms are calculated from the gravimetric data at equilibrium. Solvent partial pressures are calculated from the adsorbate temperature using the Antoine equation, with appropriate constants, for methanol (Wilhoit and Zwolinski, 1973) and tabulated data for water (Handbook of Chemistry and Physics, 1956).

Results

Calorimetry / X-ray

Heats of solution to infinite dilution, ΔH_s^0, and X-ray powder pattern results are summarized in Table 1. The heats of solution for the desolvated forms are identical. The X-ray patterns for the 4 samples are classified as 3 distinct patterns: I (methanolate), II (hydrate), and III (anhydrate). Pattern differences between methanolate and anhydrate are quite pronounced while the differences between hydrate and anhydrate are slight. Thus, both the X-ray data and the heat of solution data indicate that the desolvated methanolate and the desolvated hydrate crystals are the same polymorph, which we refer to as the anhydrate.

Desorption / absorption isotherms (Fig. 2)

In a desorption experiment with a stoichiometric solvate, one expects the solvent content to decrease only slightly, due to surface desorption, until the partial pressure of the solvent decreases slightly below the equilibrium vapor pressure of the solvated crystal, at which point the solvated crystals will be thermodynamically unstable and

TABLE 1

HEATS OF SOLUTION IN WATER FOR CRYSTALLINE FORMS OF CEFAMANDOLE SODIUM AT 25°C

Form	Heat of solution, $\Delta\bar{H}s^0$ (kcal/mol)	X-ray pattern
Methanolate	$+0.16 \pm 0.02$	I (methanolate)
Monohydrate	$+0.26 \pm 0.05$	II (hydrate)
Desolvated methanolate	-1.81 ± 0.01	III (anhydrate)
Desolvated hydrate	-1.84 ± 0.05	III (anhydrate)

complete desolvation to the anhydrate will occur without further reduction in partial pressure. Conversely, in an absorption experiment, the anhydrate will be thermodynamically stable at partial pressures below the equilibrium vapor pressure of the solvate and will surface adsorb only small quantities of solvent until the solvent partial pressure slightly exceeds the vapor pressure of the solvate, whereupon complete conversion of anhydrate to solvate will occur. Further increases in solvent partial pressure will result in only slight increases in solvent content arising from

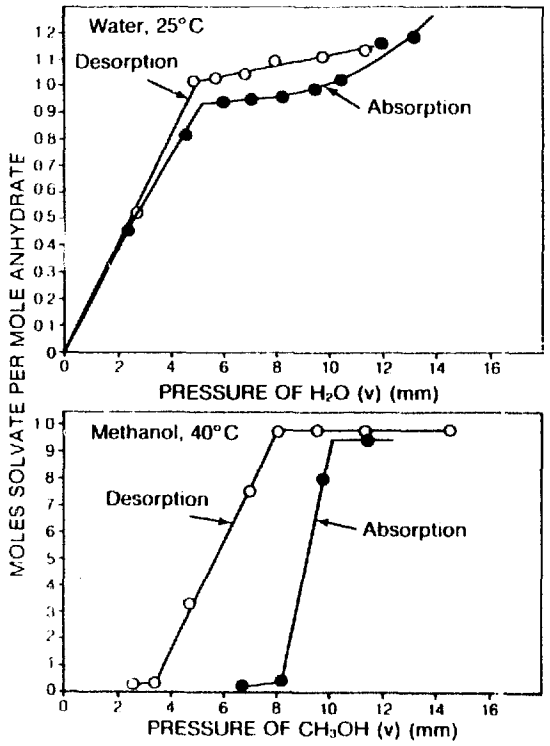

Fig. 2. Desorption and absorption isotherms for cefamandole sodium.

surface adsorption by the solvate crystals. Thus, for a classical stoichiometric solvate, the desorption/absorption isotherms are coincident, provided thermodynamic equilibrium exists, and the composition vs partial pressure curve closely resembles a step function with the discontinuity in composition occurring at the equilibrium vapor pressure of the solvate (or dissociation pressure of the solvate, P_0 (Haleblian, 1975; Findlay, 1951)). The step function behavior is a direct result of the co-existence of two distinct solid phases (i.e. the solvate and the anhydrate) and the vapor phase (Findlay, 1951).

Although there exist numerous examples of stoichiometric solvates, including several cephalosporins (Pfeiffer et al., 1970), many solvates exhibit desorption/absorption isotherms which, in shape, closely resemble surface *adsorption* isotherms (Haleblian, 1975). That is, the solvent content of the solid increases continuously from zero as the solvent partial pressure increases from zero with no sharp breaks or steps in the curve and no well-defined plateau level in composition. Solvates in this class are denoted non-stoichiometric solvates (Haleblian, 1975; Soustelle et al., 1972; Barrer and Bratt, 1960) and are regarded as a single solid phase where the solvent is present as a solid solution in the crystalline solid phase (Haleblian, 1975; Soustelle et al., 1973).

The cefamandole sodium isotherms (Fig. 2) appear to be composites of stoichiometric and non-stoichiometric solvates with the 'water' curve more closely resembling a classical non-stoichiometric solvate and the 'methanol' curve being *somewhat* closer to a stoichiometric solvate. Indeed, it appears that, on desorption, the methanolate solid phase is a non-stoichiometric solvate which persists until the solvent content decreases to near zero at a partial pressure of about 3.5 mm Hg, whereupon a phase change occurs forming the anhydrate. The lack of coincidence in 'water' desorption and absorption curves could be a consequence of capillary condensation but it seems unlikely that capillary condensation could produce the difference in desorption and absorption found in the 'methanol' curves. A possible interpretation is that in the absorption curve, below a partial pressure of 8 mm Hg, the anhydrate is metastable in the same sense as a supersaturated solution, and significant uptake of methanol does not occur until surface *adsorption* of methanol reaches a level sufficient to facilitate crystallization to the methanolate phase.

Microscopic observations

Visual observations of demethanolation in vacuum (Fig. 3) at 65°C and the methanolate to hydrate reaction at 25°C (Fig. 4) show a time-dependent darkening of the crystals (lot no. 5) which presumably represents appearance of a polycrystalline product phase (Byrn, 1976) [4]. The reaction appears to originate at the crystal edges and 'defect' locations caused by chips (Fig. 3a, center of crystal on right) or a broken end (Fig. 4a, bottom of center crystal). It is significant to note that not all crystals react at the same rate. Demethanolation in the crystals on the left in Fig. 3 is complete well in advance of the crystal on the right while conversion to hydrate (Fig.

[4] Transmitted light is used to view the samples. The polycrystalline phase reflects the light and renders the sample opaque.

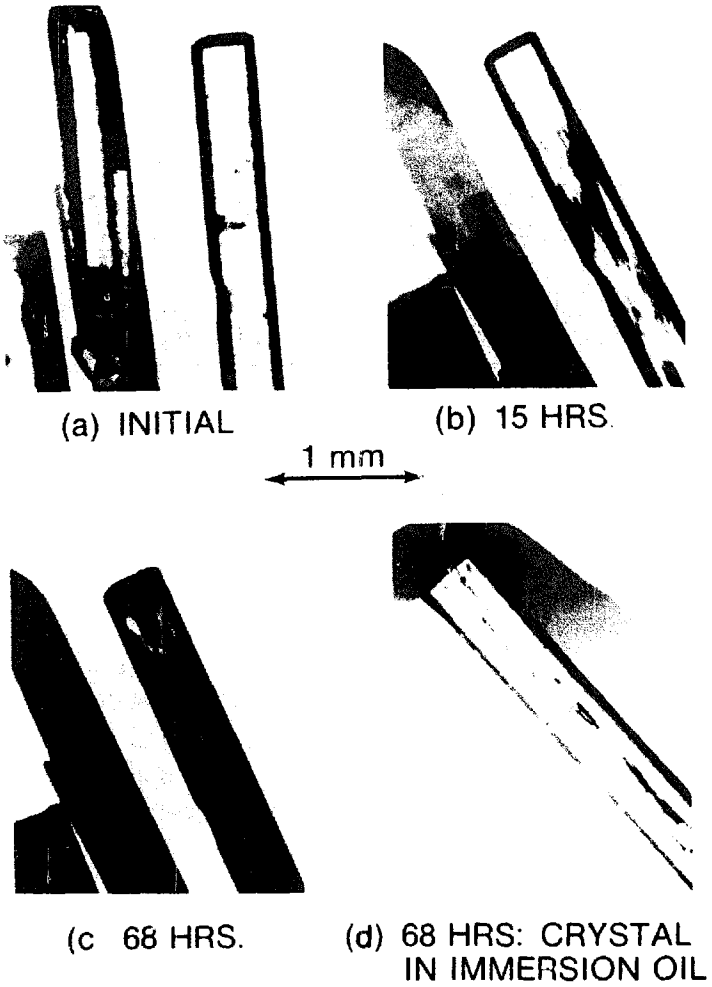

Fig. 3. Microscopic observations: sample exposed to vacuum, 65°C.

4) is much slower for the crystal in the center of the photograph than for the crystal at the top. After completion of the reaction, a crystal was placed in immersion oil and examined for cracking, which is commonly observed in solid state reactions (Kornblum and Sciarrone, 1964; Prout and Tompkins, 1944). A few large cracks are observable in the sample demethanolated in vacuum (Fig. 3c) while extensive cracking is observed for the sample converted to the hydrate (Fig. 4c). Other observations demonstrate that most of the cracking occurs within the first 10–20 min of exposure to water vapor.

Kinetic studies with cefamandole sodium

The kinetics of demethanolation in vacuum and the kinetics of the methanolate to hydrate conversion are compared for several crystal preparations in Table 2. Demethanolation in vacuum is approximately first-order where the half-life is directly proportional to the square of the crystal length. However, the methanolate to hydrate kinetics follow sigmoid kinetics typical of solid state reactions where the

half-life, defined as the time required to reach a fractional extent of reaction (α) of $\frac{1}{2}$, is much less sensitive to crystal size.

The kinetic data obtained for cefamandole sodium are summarized by Table 3. The first column identifies the experiment number. The results given for a given experiment number normally represent the mean of at least two independent experiments. The temperature (°C) is given by the second column while the crystal history is listed in the third column. A fresh crystal refers to a methanolate sample which had *not* previously been converted either to the hydrate or anhydrate. The term 'from methanolate' indicates that the starting material for that reaction (i.e. either an anhydrate or hydrate) as prepared from the methanolate. The term 'from hydrate' indicates the sample has been converted to the hydrate at one time and therefore, is a highly cracked crystalline material (Fig. 4). The fifth column gives the induction period for the reaction, t_0, defined by

$$\frac{d\alpha}{dt} > 0,\ t > t_0 \tag{9}$$

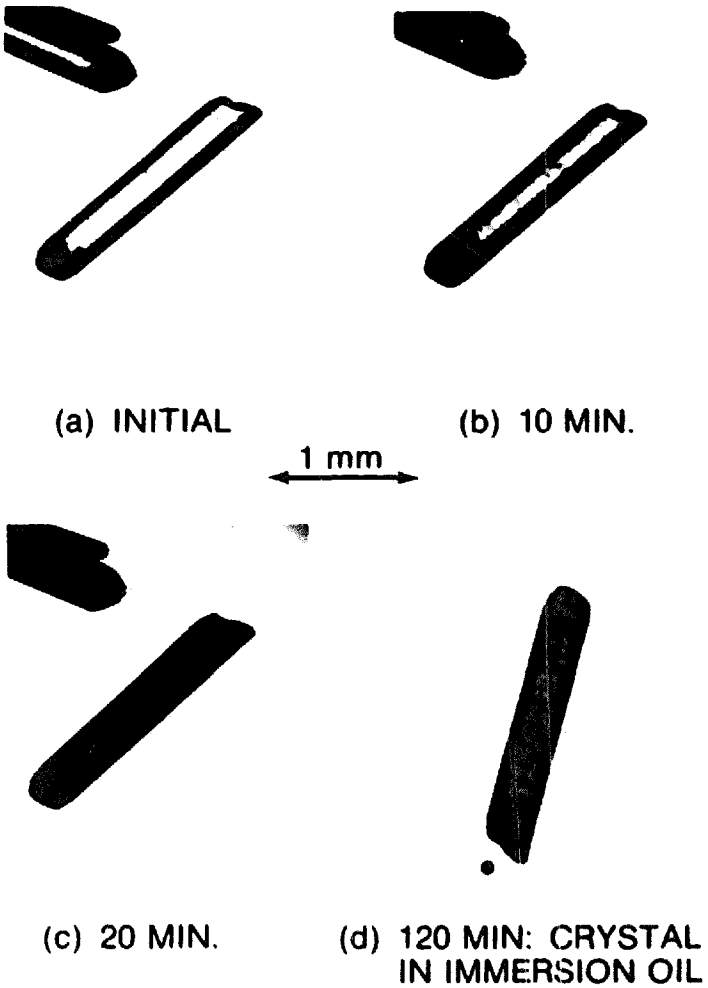

Fig. 4. Microscopic observations: sample exposed to water vapor: 25°C, 50% relative humidity.

TABLE 2

EFFECT OF CRYSTAL SIZE AND RELATIVE HUMIDITY (*R.H.*) ON DEMETHANOLATION OF CEFAMANDOLE SODIUM AT 25°C

Lot no.	Crystal length (mm) [a]	Half-life (h)	Type kinetics	Product crystal cracked?
	methanolate (crystalline) $\xrightarrow{R.H.=0}$ anhydrate (crystalline)			
1	0.3	~ 5 [b]	1st/order	–
2	1.2	27.2	1st/order	–
3	3	190	[c]	Slight
5	3	207	[c]	Slight
	methanolate (crystalline) $\xrightarrow{R.H.=44\%}$ hydrate (crystalline)			
4	0.1	0.91	Sigmoid [d]	No
2	1.2	0.56	Sigmoid [d]	Yes
3	3	2.0	Sigmoid [d]	Yes
5	3	1.58	Sigmoid [d]	Yes

[a] Crystal habit for all samples is prismatic with the ratio of the long axis (length) to the short axis being about 7. The lengths tabulated are approximate average values.
[b] Estimated from data at 40°C assuming the effect of temperature for lot no. 1 is the same as for lot no. 2.
[c] Assumed to be first-order. Data collected only to $\alpha = 0.06$.
[d] Asymetric sigmoid α vs t curve with inflection point occurring when $\alpha < 0.5$.

The half life, $t_{1/2}$, given in column 6 is taken as the time to reach $\alpha = \frac{1}{2}$. The rate, $d\alpha/dt$, at time $t_{1/2}$ is given in the last column. Note that for a first order reaction, the product of the rate at $t_{1/2}$ and the half-life is 0.346. For a sigmoid curve, this product is greater than 0.346 while for a reaction of higher order than first (i.e. a bi-exponential decay), the product is less than 0.346.

The effect of water vapor on the kinetics of demethanolation and examples of sigmoid kinetics are illustrated by Fig. 5. In vacuum, demethanolation is slow, but in the presence of water vapor, loss of methanol with subsequent formation of hydrate is very rapid and follows general sigmoid kinetics (Young, 1966). For a symmetrical sigmoid curve the rate is a maximum at $\alpha = \frac{1}{2}$. The data (Fig. 5) are describable by an asymmetric sigmoid curve where the maximum rate occurs at $\alpha < \frac{1}{2}$. The extent of reaction is defined as the mass change at any time, t, divided by the mass change at time infinity. During substitution of water for methanol, the mass change is a loss in mass, and the negative extents of reaction near time zero (Fig. 5) correspond to a measured mass *Increase*. Evidently, the sample adsorbs water vapor immediately but loss of methanol is not immediate. Rather, there is an induction period characterized by $d\alpha/dt \leq 0$, and only after the induction period does the transition from methanolate to hydrate begin. The induction period is greatly extended as the relative humidity is lowered.

Examples of first-order dehydration kinetics are shown by Fig. 6. Although there may be a very slight induction period due to the time delay in dry nitrogen passing through the flow system (Fig. 1) to the sample, the curves are essentially first-order, with the reaction rate decreasing with a decrease in temperature.

The kinetics of forming the methanolate depend strongly upon whether the

TABLE 3

SUMMARY OF KINETIC DATA FOR DESOLVATION AND SOLVATION OF CEFAMANDOLE SODIUM

Exp. no.	T (°C)	Crystal history (lot no.)	Relative humidity (%)	t_0 (h)	$t_{1/2}$ (h)	Rate at $t_{1/2}$ (h^{-1})
methanolate → anhydrate						
1	25.0	Fresh (2)	0 (vacuum)	0	27.2	0.0147 [a]
2	40.8	Fresh (2)	0 (vacuum)	0	10.1	0.0297 [a]
3	54.0	Fresh (2)	0 (vacuum)	0	6.0	0.0564 [a]
4	65.2	Fresh (2)	0 (vacuum)	0	3.21	0.105 [a]
5	40.8	Pre-nucleated w H_2O (v) (2) [b]	0 (vacuum)	0	2.0	0.080
6	40.0	Ground to powder (2) [c]	0 (vacuum)	0	0.50	0.31
7	25.0	Fresh (5)	0	0	207 [d]	0.00167 [d]
8	25.0	From hydrate (5)	0	0	3.03	0.166
anhydrate → methanolate						
9	25.0	From methanolate (2)	0 [e]	0	2.5	0.082
10	25.0	From hydrate (2)	0 [f]	0	0.55	0.61 [a]
11	25.0	From hydrate (5)	0 [f]	0	0.25	1.2 [a]
methanolate → hydrate						
12	25.0	Fresh (2)	44	0.07	0.56	1.42 [g]
13	25.0	From hydrate (2)	44	0.07	0.41	1.89 [g]
14	15.0	Fresh (2)	44	0.17	1.60 [g]	0.42 [g]
15	15.0	From hydrate (2)	44	0.17	1.25	0.65 [g]
16	25.0	Fresh (2)	10.3	0.57	1.01	1.26 [g]
17	25.0	Fresh (5)	44	0.15	1.58	0.50 [g]
18	25.0	From hydrate (5)	44	0.05	0.78	0.95 [g]
hydrate → methanolate						
19	25.0	From methanolate (2)	0 [f]	0.32	1.36	0.46
hydrate → anhydrate						
20	25.0	From methanolate (2)	0	0	0.25	1.55 [a]
21	15.0	From methanolate (2)	0	0	0.71	0.59 [a]
22	25.0	From methanolate (2)	0 (vacuum)	0	0.008	37
23	25.0	From methanolate (5)	0	0	0.50	0.72 [a]

[a] Approximately 1st-order.
[b] Exposed to 58% relative humidity at 25°C for 12 min.
[c] Crystal size ≈ 30 μm × 30 μm.
[d] Assumed to be 1st-order. Data collected only to $\alpha = 0.06$.
[e] Relative vapor pressure of methanol is 0.054.
[f] Relative vapor pressure of methanol is 0.079.
[g] Approximately sigmoid α vs t curve.

starting material is the anhydrate or hydrate (Fig. 7). The kinetics for formation of methanolate from anhydrate are higher than first-order while the kinetics for methanolate formation from hydrate show large negative α values, That is, at early times there is significant mass loss before mass gain is finally observable. It appears that nearly complete dehydration occurs before uptake of methanol and conversion to methanolate begins. Indeed, the α vs time curve for conversion of hydrate to

Fig. 5.

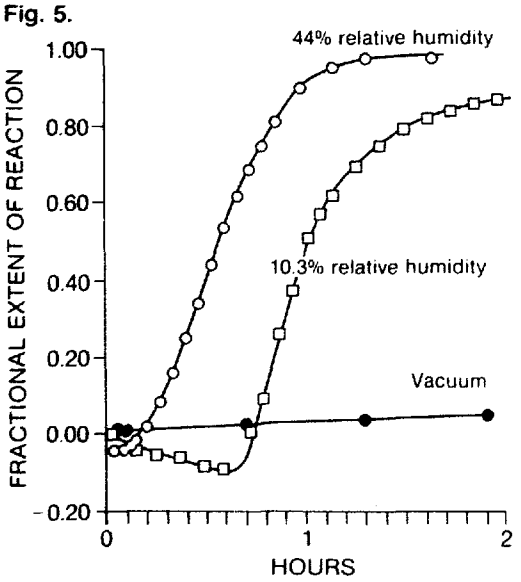

Fig. 6.

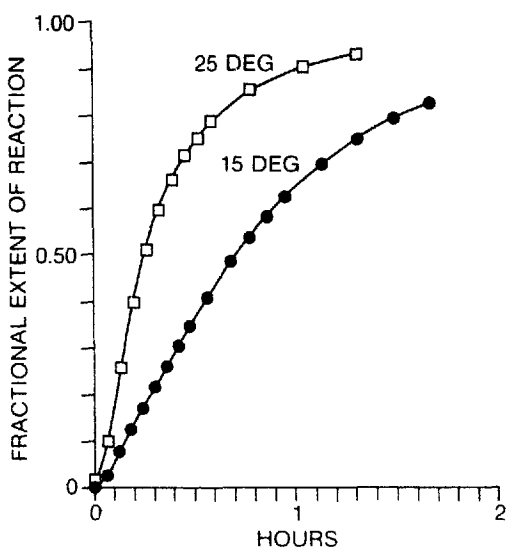

Fig. 5. Effect of water vapor on demethanolation kinetics at 25°C; sigmoid kinetics. (Fresh crystals, Lot no. 2.)

Fig. 6. Kinetics of dehydration (Lot no. 2).

Fig. 7.

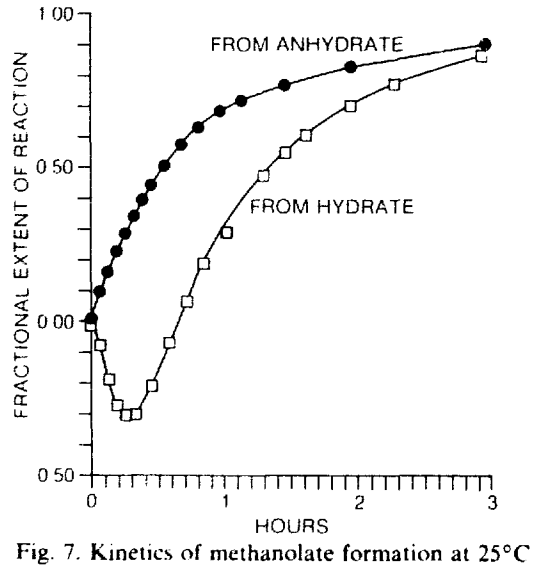

Fig. 8.

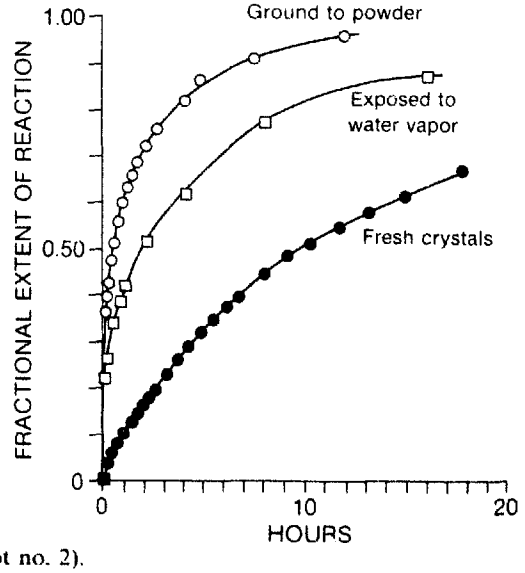

Fig. 7. Kinetics of methanolate formation at 25°C (Lot no. 2).

Fig. 8. Vacuum demethanolation at 40.8°C: effect of sample history (Lot no. 2).

methanolate can be calculated as the simple sum of dehydration according to the kinetics in Fig. 6 and methanolation of the anhydrate according to the kinetics of Fig. 7.

The first-order vacuum demethanolation of fresh crystals is compared in Fig. 8 with the higher-order kinetics found when the crystals are exposed to water vapor to cause cracking (Fig. 4) or when the crystals are ground to a fine powder. The effect of increased surface area either by cracking or by grinding, is to significantly increase the demethanolation rate, as expected from the trends with crystal size presented in Table 2.

Cefazolin sodium and cefamandole nafate

The α-form of cefazolin sodium is frequently referred to as a pentahydrate but in reality is a classical non-stoichiometric hydrate which contains about 5 moles of water at high relative humidity. The crystals are prismatic with the ratio of the long axis (length) to the short axis being about 10. The mean length is about 0.5 mm. The observations regarding removal of ethanol from the pseudo-ethanol solvate of cefazolin sodium are illustrated by Scheme II.

Cefazolin sodium (α)[1.65% Ethanol]

3 h ↓	25°C vacuum	3 h ↓	25°C 60% R.H.
1.43% ethanol		0.19% ethanol	

Scheme II

Thus, the rate of solvent removal is roughly 7 times faster in air at 60% relative humidity (R.H.) than in vacuum. No cracking is observed in either vacuum drying or in air-drying.

Desorption isotherm data suggest that the methanolate of cefamandole nafate is approximately a stoichiometric solvate. The crystals are of the same shape as cefamandole sodium methanolate but are much smaller, the mean length being only about 0.05 mm.

The results of several experiments with cefamandole nafate, denoted CN, are summarized by the following reactions:

$$\text{(F)}\quad \text{CN} \cdot \text{MeOH} \xrightarrow[25°\text{C}]{20\%\ \text{R.H.}} \text{CN} \cdot \text{H}_2\text{O}\ \text{(X-ray: methanolate)}$$

$$\text{(G)}\quad \text{CN} \cdot \text{H}_2\text{O} \xrightarrow[25°\text{C}]{\text{dry air}} \text{CN (X-ray: anhydrate, } \delta\text{)}$$

$$\text{(H)}\quad \text{CN} \cdot \text{MeOH} \xrightarrow[25°\text{C}]{\text{dry air}} \text{CN (X-ray: anhydrate, } \delta\text{)}$$

where the rate of methanol removal at 20% relative humidity (reaction F) is roughly

a factor of 5 faster than the corresponding rate at zero relative humidity (reaction H). In the presence of moisture (reaction F), the methanolate converts to a form which contains 1 mole of water but retains the methanolate structure. Removal of water yields the δ-anhydrate form which has a different X-ray pattern than the γ-anhydrate form which is prepared by crystallization from non-aqueous solution (Pikal et al., 1978). The heat of solution of the δ-form (−2.2 kcal/mole) is also quite different from the γ-form (1.9 kcal/mole) (Pikal et al., 1978) and indicates the δ-form is a high-energy anhydrate form. Removal of methanol in vacuum or dry air (reaction H) also produces the δ-form.

Discussion

Phenomenological

Nucleation and cracking

Conventional views of solid state reactions (Byrn, 1976; Carstensen, 1974; Young, 1966; Kornblum and Sciarrone, 1964; Garner, 1955; Prout and Tompkins, 1944) hold that the chemical or physical change under consideration proceeds at reactive sites, or reaction nuclei, located at the boundary between two phases. In a system of unreacted crystals, the reaction begins at defect sites on the crystal surface, which function as the initial reaction nuclei, forming product phase. The boundary between product and reactant is itself a high energy region and therefore functions as a reaction nucleus resulting in further growth of the product phase. Since the net reaction rate is proportional to the area of the product/reactant phase boundary and since this area increases as reaction proceeds in the early stages, the reaction rate initially increases with time. Frequently crystallization of the product phase results in sufficient strain to form cracks which permeate the crystal thus forming fresh surface for formation and growth of nuclei. Thus, cracking will further accelerate the reaction. As reaction proceeds and the amount of reactant phase decreases, the area of the product/reactant phase boundary will eventually decrease toward zero causing the reaction rate to decrease toward zero. These phenomena frequently, but not necessarily (Carstensen and Pothisiri, 1975), result in sigmoid kinetics.

The demethanolation of cefamandole sodium appears generally consistent with the above principles, the demethanolation in presence of water vapor being nearly a classic example complete with sigmoid kinetics. Water vapor adsorbs on the crystal surface (Fig. 5), product nuclei form at defect sites (Fig. 4b), spread over the surface of the crystal (Fig. 4c) [5], numerous cracks form, and the reaction rate increases dramatically yielding sigmoid kinetics (Fig. 5) (Table 3, Exp. 17). The induction period, t_0 increases as the temperature decreases (Table 3, Exp. 12 vs Exp. 14) as expected (Young, 1966), yielding an activation energy for nucleation of 15 kcal/mol. Further, the induction period increases dramatically as the relative humidity is

[5] The crystal (Fig. 4c) is opaque after 20 min but the half-life for this lot (no. 5) is 1.58 h (Table 3, Exp. 17). Thus, the product phase is, for the most part, confined to the surface at the 20 min time period.

decreased (Fig. 5; Table 3, Exp. 12 vs Exp. 16), suggesting that nucleation may be mediated by the presence of an adsorbed multilayer state of water on the crystal surface.

The most dramatic visual difference between demethanolation in vacuum and demethanolation in the presence of water vapor lies in the degree of crack formation (Figs. 3c and 4c). Samples exposed to water vapor are much more highly cracked and therefore have a much larger effective surface area to support the demethanolation reaction.

Effect of crystal surface area

The effective surface area of the methanolate was varied by control of the crystallization procedure (Table 2), pre-treatment of a sample by exposure to water vapor (Table 3, Exp. 5; Fig. 8), or by grinding (Table 3, Exp. 6; Fig. 8), and by complete conversion to the hydrate (producing cracked crystals) followed by reformation of the methanolate (Table 3, Exps. 8, 13, 15, 18). For each method of increasing the surface area, the rate of methanolate to anhydrate conversion is found to be much faster for the sample of higher surface area (smaller effective crystal size), the most dramatic effect being the comparison between large fresh crystals of lot no. 5 and crystals of the same lot which had previously been converted to the hydrate. Here, the demethanolation rate is accelerated by two orders of magnitude (Table 3, Exp. 7 vs Exp. 8). In general, the rate of conversion of methanolate to hydrate (i.e. methanolate in presence of water vapor) increases slightly as the crystal size of the starting material decreases [6] (Tables 2 and 3). Since the effective crystal size for the methanolate to hydrate conversion is determined largely by the cracking phenomena, the very slight dependence of reaction rate on size of the starting material is expected.

Methanolate → anhydrate vs anhydrate → methanolate

Conversion of methanolate to anhydrate is roughly first-order with a half-life of 27.2 h at 25°C (Table 3, Exp. 1) while the corresponding reverse reaction of anhydrate to methanolate exhibits higher-order kinetics and is much faster with a half-life (time to $\alpha = \frac{1}{2}$) of only 2.5 h (Table 3, Exp. 9). Thus, the solvation reaction is much faster than the desolvation reaction. Note that the rate of methanolate formation from the anhydrate is much faster for anhydrate prepared from the hydrate (Exp. 10) than for anhydrate obtained by vacuum demethanolation (Exp. 9), a result consistent with a higher surface area for highly cracked crystals (Fig. 4d) than for crystals obtained by vacuum demethanolation (Fig. 3d).

Demethanolation vs dehydration

A comparison of methanolate to anhydrate conversion with hydrate to anhydrate conversion is dominated by the difference in surface area if fresh methanolate crystals are used for the comparison. However, if the methanolate crystals are

[6] The half-life for lot no. 4 (Table 2) is anomalously long. However, this lot did not appear to crack upon reacting.

TABLE 4

APPARENT ACTIVATION ENERGIES AND HEATS OF REACTION: LOT NO. 2

Reaction	ΔE^* (kcal/mol)	$\Delta \bar{H}^0$ (kcal/mol)
methanolate → anhydrate	12.5 ± 0.2 [a]	12.66
hydrate → anhydrate	17 [b]	12.57
methanolate → hydrate	19 ± 1.2 [c]	0.09

[a] Evaluated from rate data for the same sample ($\alpha \approx 0.3$) at 25°C and 43°C extrapolated to a common time point. The pressure was maintained at 2 mm Hg to facilitate heat transfer and thereby minimize the self-cooling error.

[b] From 1st-order rate constants (h^{-1}): 0.97 (15.0°C), 2.61 (25.0°C).

[c] From $\dot{\alpha}_{1/2}$ and $t_{1/2}$; result independent of origin of data and independent of crystal history within stated uncertainty.

prepared from the *same* sample used to study the kinetics of dehydration, both methanolate and hydrate samples are 'cracked' crystals of the same surface area and geometry. Samples of lot no. 5 provide such a comparison (Table 3, Exp. 8 vs Exp. 23). Dehydration is observed to be about a factor of 5 faster than demethanolation [7].

In a study of desolvation of zeolites (Salvador and Gonzalez, 1976), it was found that removal of water was about 20 times faster at 25°C than removal of methanol, a result attributed to faster diffusion of the smaller water molecule in the crystal lattice. A similar interpretation may be applicable to desolvation of cefamandole sodium.

Demethanolation: anhydrate formation vs hydrate formation

Demethanolation of fresh crystals in vacuum or dry air forming anhydrate is much slower than demethanolation in the presence of water vapor forming hydrate. However, most of this effect may be attributed to the larger surface area during hydrate formation caused by crystal cracking. The effect of crystal cracking may be eliminated by comparing the kinetics for the following reaction sequence with the same sample: (a) hydrate formation from fresh crystals, $t_{1/2} = 1.58$ h (Table 3, Exp. 17): (b) anhydrate formation using methanolate prepared from the hydrate formed in (a), $t_{1/2} = 3.03$ h (Table 3, Exp. 8); and (c) hydrate formation using methanolate prepared from the product in (b), $t_{1/2} = 0.78$ h (Table 3, Exp. 18). Assuming that degree of cracking for reaction (b) above is approximated by the mean of that for the sample in (a) and (c), the half-life of hydrate formation for a sample comparable to the sample in (b) is given by the mean of reactions (a) and (c), or 1.18 h. Thus, hydrate formation is about a factor of 2.5 faster than anhydrate formation when the starting material is identical in effective surface area.

Temperature dependence

The apparent Arrhenius activation energies, ΔE^*, calculated from the data in

[7] Due to self-cooling effects for the very rapid dehydration, the difference between dehydration and demethanolation may be slightly larger.

Table 3 are compared with the enthalpy change for the corresponding reactions in Table 4. The enthalpy changes were evaluated from the heat of solution data (Table 1) and literature data for heat of solution of methanol in water (Arnett and McKelvey, 1966), heat of vaporization of methanol (Wilhoit and Zwolinski, 1973) and heat of vaporization of water (Handbook of Chemistry and Physics, 1956). The activation energy for the hydrate to anhydrate reaction may be slightly higher than that of the value given in Table 4 due to self-cooling effects.

While the activation energies for dehydration and methanolate to hydrate conversion are significantly higher than the enthalpy of reaction, the apparent activation energy and enthalpy of reaction are essentially identical for the methanolate to anhydrate reaction. The concept of activation energy requires the activation energy to be significantly greater than the enthalpy of reaction if formation of the activated state is the rate-determining step for conversion of the methanolate phase to the anhydrate phase. Thus, the data (Table 4) indicate that the phase change itself (methanolate → anhydrate) is not rate limiting, at least for the large fresh crystals used to evaluate the *apparent* activation energy. Rather, it appears that perhaps demethanolation of large crystals in vacuum is limited by *mass transfer* of methanol vapor through the anhydrate phase.

Mechanistic

Time dependence and mechanistic information

Although the analysis of the time dependence of the extent of reaction is a powerful method for developing mechanistic information on reactions in solution or the gas phase, such methodology is far less informative when applied to reactions in solids. Non-uniformity of crystal size and defects in a powder sample, alteration of crystal size and shape during the reaction by cracking, and the possibility of different reaction rates for the different crystal faces (Byrn, 1976) are all complicating factors not adequately accounted for in the usual mathematical models (Carstensen, 1974) for solid state reactions. Even for crystals of uniform and well-defined geometry, a solid state mechanism involving nucleation and growth of product nuclei can lead to kinetics ranging from sigmoid to first-order (Carstensen and Pothisiri, 1975).

The kinetics of vacuum demethanolation over the entire α (extent of reaction) range are best described by first-order kinetics, although the contracting sphere or contracting cylinder models (Carstensen, 1974) fit nearly as well, and the data from $\alpha = 0.15$ to $\alpha = 0.9$ are fit extremely well by the contracting cylinder diffusion model (Jander equation) (Carstensen, 1974). The methanolate to hydrate reaction yields kinetics best described by a modified Prout-Tompkins (Carstensen, 1974; Prout and Tompkins, 1944) model [8], but a model based on water adsorption followed by first-order demethanolation kinetics after an induction period fits the data nearly as well. Thus, mechanistic interpretations resulting from analysis of the time depen-

[8] The Prout-Tompkins model was modified by removing the usual assumption that the initial number of nucleation sites is negligible and by allowing for mass changes resulting from water adsorption.

dence of α are ambiguous. However, some mechanistic information may be revealed by an analysis of the phenomenological trends in the data discussed in the preceding section within the framework of a general theoretical model.

A theoretical model for mass transfer-limited desolvation

The proposed model involves rapid equilibrium between solvate and anhydrate at the boundary between the two phases where the equilibrium vapor pressure of the solvate is P_0. The rate-determining step is vapor flow through the anhydrate phase by means of either Knudsen flow or surface diffusion. With Knudsen flow, the resistance to mass transport arises from diffuse scattering of the gas molecules from a solid surface and depends on temperature only through the square-root of absolute temperature (Barrer, 1948, 1963). The solid surface refers to the 'pore walls' of the micropores in the polycrystalline anhydrate phase. Surface diffusion (Barrer, 1948, 1963) refers to a mass transport mechanism where the gas molecule moves by discrete translational 'jumps' between adsorption sites on the pore walls and is an activated process in the sense that the temperature dependence of the mass transfer coefficient is described by the Arrhenius relationship.

The model assumes a sharp boundary between solvated and desolvated phase where the partial pressure of the solvent decreases linearly from P_0 at the boundary to zero at the crystal surface. Since the only time dependence in the model is in the movement of the boundary, Fick's first law may be used to describe the flux, J ($mol/cm^2 \cdot s$),

$$J = -D\frac{\partial c}{\partial x} \tag{10}$$

where c is the concentration of gas in the anhydrate phase, and D is the mass transfer coefficient. Assuming ideal gas behavior and a constant pressure gradient gives

$$-\frac{\partial c}{\partial x} = \frac{\epsilon P_0}{RTx} \tag{11}$$

where ϵ is the void volume fraction in the anhydrate phase, R is the gas constant, T is the absolute temperature, and x is the thickness of the desolvated region at time t. If n_0 and n represent the number of moles of solvent in the crystal at time zero and time t, respectively, the fractional extent of reaction, α, is given by the ratio, n/n_0. Thus, the molar flux, J, is given by

$$J = \frac{n_0}{A(x)} \cdot \frac{d\alpha}{dx} \cdot \frac{dx}{dt} \tag{12}$$

where A(x) is the area of the solvate/anhydrate reaction boundary which, in general,

is a function of the thickness of the anhydrate phase, x. Combination of Eqns. 10–12 yields

$$x \cdot \frac{dx}{dt} = \frac{D\epsilon P_0}{RT} \cdot \left[\frac{A(x)dx}{n_0 d\alpha} \right] \tag{13}$$

Since the differential change in reacted volume, dv, is equal to both A(x)dx and $v_0 d\alpha$, where v_0 is the crystal volume, the term in Eqn. 13 enclosed by brackets is simply, $1/c_0$, where c_0 is the initial molar concentration of solvent in the crystal. Thus, integration of Eqn. 13 yields the time dependence of x.

$$x^2 = \frac{2D\epsilon P_0}{c_0 RT} t \tag{14}$$

Eqn. 14 applies to any regular crystal geometry (i.e. slab, cylinder, sphere) but the functional relationship between extent of reaction and x, $\alpha(x)$, depends on the crystal geometry. For a slab of thickness 2a, $\alpha(x) = x/a$, but for spherical and cylindrical geometry the relationship is more complex (Carstensen, 1974). In general, taking 'a' to represent the value of x when the desolvation is complete, and introducing the definition, $z = (x/a)^2$ allows the time required for 50% completion of the reaction, $t_{1/2}$, and the reaction rate at $t_{1/2}$, $\dot{\alpha}_{1/2}$, to be expressed in general form,

$$t_{1/2} = K_1 \frac{c_0 RT}{2\epsilon D} \frac{a^2}{P_0} \tag{15}$$

$$\dot{\alpha}_{1/2} = K_2 \frac{2\epsilon D}{c_0 RT} \frac{P_0}{a^2} \tag{16}$$

where K_1 and K_2 are numerical constants, specific to the crystal geometry, representing the values of z and $(d\alpha/dz)$, respectively, at $\alpha = \frac{1}{2}$. The parameter, a, is a crystal size parameter whose precise meaning depends on the geometry of the reaction interface. For a slab, a is the half-thickness while for a cylinder reacting radially, a is the radius of the cylindrical crystal. The value of the product, $\dot{\alpha}_{1/2} \cdot t_{1/2}$, depends on the reaction geometry alone and is 0.31 for spherical geometry, 0.25 for slab geometry, and 0.21 for cylindrical geometry.

The apparent activation energy, ΔE^*, is determined by differentiation of Eqn. 16 with respect to temperature and for Knudsen flow where $D \propto T^{-1/2}$ (Dushman, 1962), is

$$\Delta E^* = \Delta \bar{H}^0 - \tfrac{1}{2}RT \quad \text{(Knudsen Flow)} \tag{17}$$

while if vapor flow involves activated surface diffusion with activation energy E_D^*, the result is

$$\Delta E^* = \Delta \bar{H}^0 - RT + E_D^* \quad \text{(surface diffusion)} \tag{18}$$

In both Eqns. 17 and 18, $\Delta\bar{H}^0$ is the enthalpy of reaction arising from the temperature dependence of P_0.

Interpretation of observations

The crystal size effect noted for vacuum demethanolation is found experimentally to be approximately an inverse proportion between reaction rate and square of crystal size, in agreement with the theoretical result (Eqn. 16).

The experimental result for vacuum demethanolation, $\Delta\bar{H}^0 \sim \Delta E^*$, is also in agreement with the mass transfer theory, provided the mass flow mechanism is Knudsen flow (Eqn. 17), since RT is small (0.6 kcal/mol).

In terms of the theory, dehydration is limited by activated surface diffusion of water through the anhydrate phase (i.e. $\Delta E^* > \Delta\bar{H}^0$). This conclusion is suspect, however, since dehydration in vacuun is much faster than dehydration in dry air (Table 3, Exp. 20 vs Exp. 22), suggesting that dehydration is limited by gas phase diffusion within the *void space* between crystals—which is not an activated diffusion process (Dushman, 1962). The interpretation of this anomaly is not immediately obvious.

For crystals of the same size and geometry, the desolvation rate is proportional to the product of the mass transfer coefficient, D, and the equilibrium vapor pressure of the solvate, P_0 (Eqn. 10). Assuming that P_0 may be taken as the mean pressure during the desolvation portion [9] of the desorption isotherm (Fig. 2), and using the enthalpy of demethanolation (Table 4) to extrapolate the methanol data to 25°C, the values of P_0 are 2.06 mm Hg for the methanolate and 2.5 mm Hg for the hydrate. These P_0 values and the rate data for desolvation of cracked crystals (Table 3, Exp. 8 and Exp. 23) may then be used to calculate the ratio, $D_{H_2O}/D_{CH_3OH} = 3.6$. If *both* dehydration and demethanolation rates were limited by gas phase diffusion in the void space between crystals, this ratio would represent the ratio of diffusion constants of water and methanol in air, which may be estimated from kinetic theory (Dushman, 1962) as 1.33. Thus, it does not appear that *both* desolvation rates are limited by diffusion of the vapors in air. The experimental ratio (3.6) does appear to be consistent with the speculation that demethanolation is limited by Knudsen flow while dehydration proceeds mainly by surface diffusion.

Since mass transfer during formation of methanolate from anhydrate proceeds through the methanolate structure, size exclusion of methanol from the anhydrate is not a factor. Consistent with the partial non-stoichiometric character of the methanolate solvate and the relatively small enthalpy of solvation (only 3.7 kcal/mole greater than the enthalpy of condensation for methanol), one might postulate a significant degree of freedom of translational motion for the solvated methanol. Thus, rapid diffusion of methanol through the methanol solvate might be expected which, of course, is consistent with the relatively rapid rate of formation of methanolate from the anhydrate.

The conversion of methanolate to hydrate is faster than conversion of methano-

[9] The desolvation portion of the isotherm is the portion of the desorption isotherm where the solvent content decreases sharply with decreasing pressure.

late to anhydrate even when data on crystals of the same surface area (effective size) are compared. Qualitatively, the same observation is valid for the methanolate of cefamandole nafate and the pseudo-ethanolate of cefazolin sodium. Since for both reactions, the alcohol must be transported through the microcrystalline product phase, it appears that the hydrate phase is more permeable to alcohol than is the anhydrate phase. Perhaps the presence of water maintains the open solvent channels or cavities characteristic of the solvated crystal such that interdiffusion of water and alcohol is possible, and mass transfer can proceed at a rapid rate through the crystal structure. Indeed, as suggested by the sigmoid kinetics, hydrate formation may not be limited by mass transfer but may be limited by the rate of the phase change itself, a speculation consistent with rapid interdiffusion.

Process implications

In vacuum desolvation, the rate of solvent removal is very sensitive to crystal size, prior exposure to water, and crystal defects arising from sample handling. Thus, the reproducibility of a production desolvation process via vacuum-drying may be subject to significant lot-to-lot variation. For large crystals having characteristically long desolvation times, the reproducibility problem would be most acute. In such cases, fluid bed-drying would offer an attractive alternative. Removal of alcohol could be accomplished quickly and reproducibility by passing humidified air through the sample yielding the hydrate. Dehumidified air could then be used to quickly dehydrate the sample. Alternately, large crystals could be milled to reduce crystal size, thereby increasing the desolvation rate in a vacuum-drying process.

Conclusions

The rate of vacuum demethanolation of cefamandole sodium is limited by mass transfer of the methanol through the low permeability, polycrystalline anhydrate phase. The rate increases sharply as the crystal size of the methanolate decreases. The much faster rate of conversion of methanolate to hydrate is mostly a result of the extensive crystal cracking and subsequent increase of surface area, which occurs during the early stages of hydrate formation. However, it also appears that the hydrate phase is more permeable to alcohol than is the anhydrate phase.

References

Anous, M.M.T., Bradley, R.S. and Colvin, J., The rate of dehydration of chrome alum. J. Chem. Soc., (1951) 3348–3354.

Arnett, E.M. and McKelvey, D.R., Enthalpies of transfer from water to dimethyl sulfoxide for some ions and molecules. J. Am. Chem. Soc., 88 (1966) 2598–2599.

Barrer, R.M., Diffusion in porous media. Appl. Mat. Res., 2 (1963) 129–143.

Barrer, R.M., Fluid flow in porous media. Disc. Faraday Soc., 3 (1948) 61–72.

Barrer, R.M. and Bratt, G.C., Nonstoichiometric hydrates. I. Sorption equilibriums and kinetics of water loss for ion-exchanged near-faujasites. Phys. Chem. Solids, 1Z (1960) 130–145.

Birks, J. and Bradley, R.S., The rate of evaporation of droplets. II. The influence of changes of temperature and of the surrounding gas on the rate of evaporation of drops of di-*n*-butyl phthalate. Proc. Roy. Soc. A, 198 (1949) 226–239.

Byrn, S.R., Mechanisms of solid-state reactions of drugs. J. Pharm. Sci., 65 (1976) 1–22.

Carstensen, J.T., Stability of solids and solid dosage forms. J. Pharm. Sci., 631 (1974) 1–14.

Carstensen, J.T. and Pothisiri, P., Decomposition of *p*-aminosalicylic acid in the solid state. J. Pharm. Sci., 64 (1975) 37–44.

Dushman, S., Scientific Foundations of Vacuum Technique, 2nd Edn., revised by members of the research staff of the General Electric Research Laboratory, J.M. Lafferty (Ed.), John Wiley and Sons, New York, 1962, pp. 1–48.

Findlay, A., The Phase Rule, 9th Edn., revised by A.N. Campbell and N.O. Smith, Dover Publications, 1951, pp. 212–232.

Garner, W.E., The kinetics of endothermic solid reactions. In Garner, W.E. (Ed.), Chemistry of the Solid State, Academic Press, 1955, pp. 213–231.

Haleblian, J.K., Characterization of habits and crystalline modification of solids and their pharmaceutical applications. J. Pharm. Sci., (1975) 1269–1288.

Handbook of Chemistry and Physics, 38th Edn., Chemical Rubber Publishing, Cleveland, OH, 1956.

Kornblum, S.S. and Sciarrone, B.J., Decarboxylation of *p*-aminosalicylic acid in the solid state, J. Pharm. Sci., 53 (1964) 935–941.

Pfeiffer, R.R., Yang, K.S. and Tucker, M.A., Crystal pseudopolymorphism of cephaloglycin and cephalexin. J. Pharm. Sci., 59 (1970) 1809–1814.

Pikal, M.J., Lukes, A.L., Lang, J.E. and Gaines, K., Quantitative crystallinity determinations for β-lactam antibiotics by solution calorimetry: correlations with stability. J. Pharm. Sci., 67 (1978) 767–773.

Pikal, M.J., Shah, S., Senior, D. and Lang, J.E., Physical chemistry of freeze drying: measurement of sublimation rates for frozen aqueous solutions by a microbalance technique. J. Pharm. Sci., 72 (1983) 635–650.

Prout, E.G. and Tompkins, F.C., The thermal decomposition of potassium permanganate. Trans. Farad. Soc., 40 (1944) 488–498.

Salvador, P. and Garcia Gonzalez, M.L., Macroscopic diffusion of methanol in a sodium and a decationated Y-zeolite. J. Colloid Interface Sci., 56 (1976) 577–585.

Soustelle, M., Gardet, J. and Guilhot, B., Thermodynamics of crystalline hydrates. Stoichiometry. Semin. Chim. Etat Solide, No. 6, 33 (1971–1972) (Published 1973) 33–50. From Chem. Abstr., 78 (1973) 164822f.

Soustelle, M., Jean, J. and Guilhot, B., Divarient equilibriums between hydrates and water vapor. Formulation by structure elements. C.R. Acad. Sci., Ser. C, 274 (1972) 2066–2069. From Chem. Abstr., 77 (1972) 144403w.

Wilhoit, R.C. and Zwolinski, B.J., Physical and thermodynamic properties of aliphatic alcohols, J. Phys. Chem., reference data, 2 (Suppl. 1) (1973) p. 42.

Young, D.A., Decomposition of Solids, Pergamon Press, New York, 1966, pp. 1–109.